ARTICLES

Excited-State Double Proton Transfer in 1*H*-Pyrazolo[3,4-*b*]quinoline Dimers

Joost S. de Klerk,[†] Arjen N. Bader,[†] Szczepan Zapotoczny,*[,‡] Monika Sterzel,[‡] Mariusz Pilch,[‡] Andrzej Danel,[§] Cees Gooijer,[†] and Freek Ariese[†]

Analytical Chemistry & Applied Spectroscopy, Laser Centre Vrije Universiteit Amsterdam, The Netherlands, Department of Chemistry, Jagiellonian University, Ingardena 3, 30-060 Krakow, Poland, and Department of Chemistry, Agricultural University of Krakow, Al. Mickiewicz 24/28, Krakow, 30-059, Poland

Received: September 30, 2008; Revised Manuscript Received: March 16, 2009

Pyrazoloquinolines are highly fluorescent, both in liquid solutions and in the solid state, which makes them good candidates for various optical devices. The aim of the current work is to understand the photochemical behavior of pyrazolo[3,4-*b*]quinoline (PQ), which is quite complicated since in *n*-alkane solvents PQ tends to form strong complexes with protic solvent constituents (often present as minor impurities), as well as dimers. Both types of H-bond complexes were studied systematically by temperature-dependent conventional absorption and fluorescence spectroscopy; the effect of protic solvent constituents was mimicked by varying the ethanol concentration in *n*-octane in the range from 0.0 to 0.8%. At room temperature the PQ:ethanol association constant was estimated at 80 M^{-1} and the dimerization constant at 2×10^3 M^{-1}. Dimer formation is enhanced upon lowering the temperature in pure *n*-alkane down to 220 K, and the fluorescence is strongly reduced since the dimer is nonfluorescent. Surprisingly, when irradiating a frozen sample for several minutes at very low temperatures (<40 K), a narrow-banded Shpol'skii-type fluorescence spectrum gradually appears. To explain this unusual photochemical behavior, PQ and its deuterated analogue were studied using low-temperature absorption and fluorescence spectroscopy over the 300−5 K temperature range. In the case of normal (protonated) PQ, very fast excited-state intermolecular double proton transfer is responsible for the efficient quenching of PQ dimer fluorescence. Deuteration significantly slows down this proton transfer process, and in that case under cryogenic conditions a fluorescent dimer is observed. Photoirradiation under cryogenic conditions leads to molecular rearrangement of the dimers and the appearance of monomer spectra. For both *H*-PQ and *D*-PQ, these processes were found to be reversible. A simplified reaction scheme, in which the excited tautomeric dimer plays a crucial role, is presented to explain the observations.

Introduction

The relevance of pyrazoloquinolines—compounds composed of fused quinoline and pyrazolo rings—in various chemical disciplines has been amply demonstrated, as summarized in a recent paper by Zapotoczny et al.[1] Already in 1928, pyrazolo[3,4-*b*]quinoline (denoted here as PQ) was synthesized by Musierowicz and co-workers.[2] Since then, several new derivatives of PQ have been synthesized and characterized.[3] Pyrazoloquinolines are highly fluorescent in liquid solvents as well as in the solid state. This property makes them good candidates for several optical devices. Examples are brightly fluorescent molecular sensors[4] and organic light emitting diodes (OLEDs).[5] Since in such setups PQ is a solute in a liquid solution or in a solid matrix, it is important to acquire detailed information about its photochemical and photophysical properties. It should be noticed that because of its heteroatomic character (see Figure 1), PQ is expected to interact strongly with protic solution constituents and also to form H-bonded dimers. Such a behavior has been reported for 7-azaindole (7-AI, see Figure 1), a compound with some structural similarity to PQ; 7-AI is known to interact strongly with water[6] and furthermore to form strong H-bonded dimers, which are regarded as a model for H-bonding interactions in DNA base pairs.[7]

In principle there are three tautomeric forms of PQ, as depicted in Figure 1. Their properties were studied both spectroscopically and theoretically[1,8] with emphasis on the monomeric forms 1*H*-PQ and 2*H*-PQ (see Figure 1). From previous theoretical studies it is known that 1*H*-PQ is energetically most favorable. The ground-state energy of 2*H*-PQ is about 3000 cm^{-1} higher than for 1*H*-PQ (as calculated by Zapotoczny and colleagues), whereas 9*H*-PQ is energetically extremely unfavorable and therefore not considered here at all.[1,8] Based on the Boltzmann distribution, the 3000 cm^{-1} energy difference implies that at room temperature virtually all molecules would be in the most stable 1*H* tautomeric form and that would be even more so at lower temperatures. Nevertheless, temperature-dependent absorption measurements in *n*-octane showed the dynamic equilibrium of two species. A specific solvent−solute interaction that would lead to stabilization of the 2*H*-PQ tautomer was proposed to explain the results.[1]

Alternatively, one could imagine that even the presence of a very minor amount of protic solvent in the sample might be responsible for a second PQ species, provided that its H-bonded

[†] Laser Centre Vrije Universiteit Amsterdam.
[‡] Jagiellonian University.
[§] Agricultural University of Krakow.

10.1021/jp8086545 CCC: $40.75
Published on Web 04/13/2009

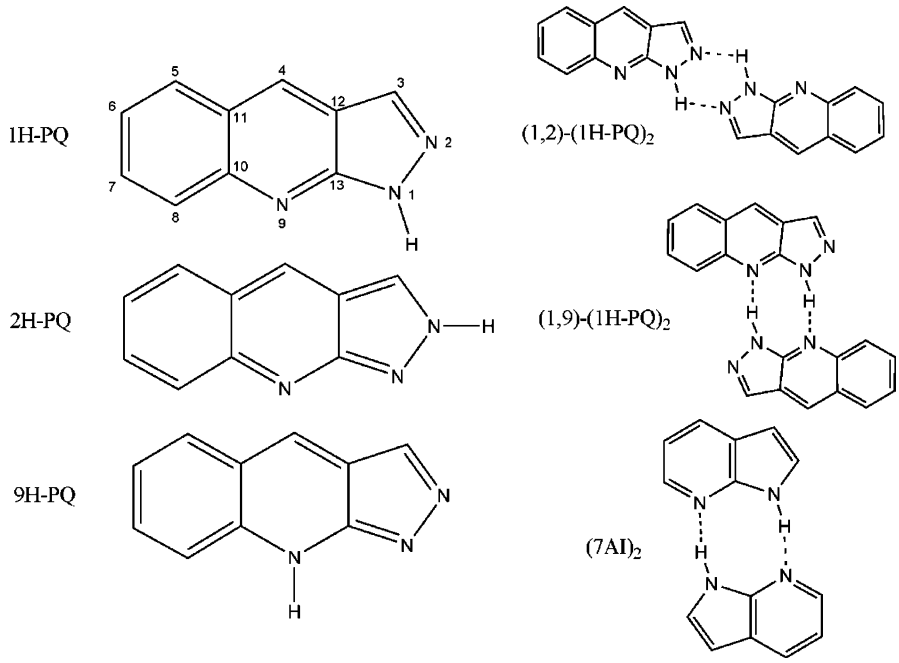

Figure 1. Structure of the three tautomeric forms of pyrazolo[3,4-*b*]quinoline, two possible dimeric structures of 1*H*-PQ, and the dimer of 7-azaindole for comparison.

interaction is very strong; a similar problem has been reported in a supersonic jet study on a reactive and a nonreactive 7-AI dimer: "the presence of H_2O could not be fully excluded".[6]

The current work focuses on the effect of H-bonding interactions on the photochemical and photophysical properties of PQ. Dimers and PQ−ethanol complexes in *n*-octane are studied in detail; the latter are used to mimic the influence of minor amounts of protic solvents possibly present as impurities in the sample. Possible dimer structures of 1*H*-PQ involving the N2 or the N9 atoms for hydrogen bonding, respectively, are included in Figure 1. As will be discussed below, the former dimer is much more favorable than the latter.

It will be shown below that the tendency of PQ to form H-bonds, either with ethanol or via dimerization, can be studied by conventional absorption and fluorescence excitation/emission spectroscopy and in more detail under cryogenic conditions. By applying high-resolution Shpol'skii-type fluorescence spectroscopy at 5 K[9] and studying the influence of deuteration, evidence is provided that PQ forms dimers that undergo excited-state double proton transfer (ESDPT), similar to dimers of 7-AI.[10] Surprisingly, the tautomeric PQ dimer is nonfluorescent, but it is gradually converted to a fluorescent species when irradiated at very low temperatures. The aim of this work is to present a complete picture of the photophysical and photochemical behavior of PQ in an *n*-alkane environment.

Experimental Section

Materials. Pyrazolo[3,4-*b*]quinoline (PQ) was synthesized and purified according to the method previously described.[11] The solvents *n*-octane (Fluka), *n*-hexane (spectroscopic grade, Sigma-Aldrich), and D_2O (Aldrich) were used as received (GC analysis of the alkanes did not show the presence of protic impurities). Deuteration of the N−H group of PQ was achieved by adding the same volume of D_2O to a PQ solution in *n*-octane, vigorously shaking the two-phase system, and letting the sample reequilibrate for three days. The upper layer (deuterated PQ in *n*-octane) was then taken for analysis. The same procedure was carried out with H_2O (milli-Q grade) as control. No additional purification steps were applied to any of the samples.

Apparatus. The standard absorption spectra at room temperature were measured with a Cary 50 spectrophotometer (Varian, Palo Alto, CA) with a spectral bandwidth of 1.5 nm, using a 1 cm quartz absorption cuvette. For the absorption spectra at different temperatures from room temperature to 200 K we used a homemade absorption setup. The sample holder consisted of two cylindrical cells of 7 mm diameter and 5 mm optical path length with sapphire windows on both sides. They were used for the sample and the solvent blank (reference), respectively. The samples were cooled by a Cryodine 21 closed-cycle helium refrigerator (CTI Cryogenics, Waltham, MA), which can be operated over a temperature range of room temperature to 14 K. The light source—a D_2 lamp (Hamamatsu Photonics, Japan), emitting from the UV to 520 nm—was focused on the lower part of the reference or sample (spot size typically 3−4 mm), thus avoiding a bubble that is formed during the cooling process (the volume of *n*-octane reduces with decreasing temperature). Detection was performed with a Shamrock monochromator model SR-303i-A and CCD camera model DV420-OE (both from Andor Technology, Belfast, U.K.). The spectra were corrected for lamp profile and scattering by consecutive measurements of the sample and the blank. At each temperature a separate reference measurement was performed. The absorption spectra were obtained in the wavelength range from 220 up to 400 nm with a spectral resolution of about 0.8 nm for the 300 lines/mm grating. Liquid-phase spectra were recorded using 30 times 0.05 s signal accumulation.

The fluorescence excitation and emission spectra at room temperature were recorded using a luminescence spectrometer LS-50B (Perkin-Elmer, Waltham, MA) with a 1 cm fluorescence quartz cuvette and a scan speed of 100 nm/min. The spectral bandwidths in excitation and emission were typically 5 nm. Spectra were corrected for the differences in excitation intensity (reference photomultiplier).

The equipment used for the broad-banded and high-resolution fluorescence measurements at different temperatures has been described in detail before.[12] This setup can be used for the measurement of liquid phase as well as frozen samples. Note that the absolute values of the fluorescence signals of crystalline

solid phase and liquid phase cannot be compared directly, because of the scattering properties of the crystalline matrix and resulting differences in optical path length and probed volume. However, the relative peak heights in the spectra can be used for comparison.

Briefly, a homemade sample holder was mounted on top of a closed-cycle helium refrigerator SRDK-205 Cryocooler (Janis Research Company, Wilmington, MA). Four samples in 2 mm internal diameter quartz tubes with a volume of approximately 100 μL and sealed with a septum could be measured separately. The excitation source was a XeCl excimer laser LPX 110i pumping a dye laser LPD 3002 (both from Lambda Physik, Göttingen, Germany). The laser system was operated at 10 Hz, producing 10 ns pulses. DMQ (Radiant Laser Dyes, Wermelskirchen, Germany) and BiBuQ (Lambda Physik) were used as laser dyes so that the excitation wavelength could be varied between 340 and 400 nm (typical output 10 mW). For nonselective excitation, a fraction of the 308 nm output of the excimer laser was used, with a typical output of a few milliwatts. The fluorescence emission was collected by two 9 cm, *f*/1.5 quartz lenses at an angle of 90° with respect to the laser beam and focused on a Spex 1877 0.6 m triple monochromator (Edison, NJ). The spectral resolution was 1 nm for the broad-banded emission in the 200−300 K range and 0.1 nm for the high-resolution measurements at low temperatures; the total detection window was 36 nm. For detection an intensified CCD camera (iStar, Andor Instruments, Belfast, U.K.) was used, operated in the gated mode to reject stray and scattered light. The camera was triggered by a trigger diode (Thorlabs DET210, Karlsfeld, Germany). In order to ensure correct timing, light from the same pulse was used for triggering; the excitation beam was then delayed by means of a 50 m optical fiber before irradiating the sample. For wavelength calibration an Fe hollow cathode lamp (Perkin-Elmer) was used.

Results and Discussion

H-Bonding Complexes of PQ. To mimic the influence of possible protic sample constituents, minor traces of ethanol were stepwise added to the PQ solution in *n*-octane. As can be seen in Figure 2A, the addition of traces of ethanol as low as 0.2% affects the absorption spectrum dramatically. In pure *n*-octane at room temperature, the longest wavelength peak in the absorption spectrum is found at 368 nm (Figure 2). Upon addition of traces of ethanol, an additional band at 378 nm shows up, and furthermore the band at 318 nm increases and shifts slightly to the red. Isosbestic points can be observed in the spectra.

In Figure 2B the temperature influence on the absorption spectra is shown for PQ in pure *n*-octane. It is striking that cooling and addition of ethanol have very similar effects on the spectra. For *n*-hexane solutions a similar temperature dependency was obtained (not shown).

The additional bands in the spectra indicate that new species are formed. The striking similarity between the effect of adding traces of ethanol and lowering the temperature suggests that the species created in either case are very similar. Most likely, these red-shifted species are PQ molecules that are H-bonded to either ethanol (Figure 2A) or to another 1*H*-PQ (Figure 2B), since in the latter case no protic solvent constituents were added. The increase in absorption at 378 nm upon adding ethanol can be fitted with an equilibrium constant for the PQ:ethanol complex: $K = [\text{PQ:ethanol}]/([\text{PQ}] \times [\text{ethanol}]) = 8 \times 10^1\ \text{M}^{-1}$ and its extinction coefficient $\varepsilon = 3 \times 10^3\ \text{M}^{-1}\ \text{cm}^{-1}$. The room temperature spectrum of PQ in *n*-octane (and *n*-hexane) in ref 1 shows already the band at 378 nm; in view of the dramatic effects caused by ethanol as shown in Figure 2A, this may be ascribed to the presence of minor traces of protic solvent constituents (origin unknown).

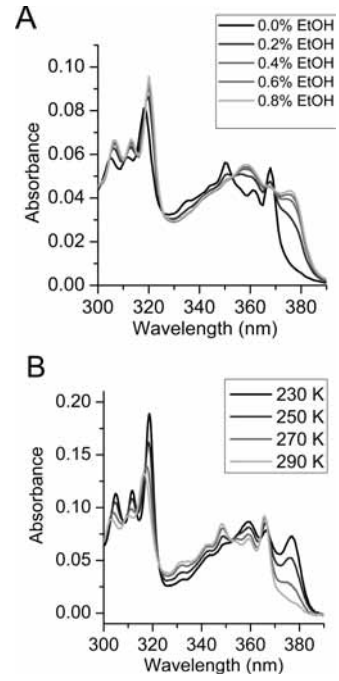

Figure 2. Absorption spectra of PQ in *n*-octane, (A) as a function of the added amount of ethanol at room temperature (concn $1.5 \cdot 10^{-5}$ M, $l = 1$ cm) and (B) as a function of temperature (concn $5 \cdot 10^{-5}$ M, $l = 0.5$ cm).

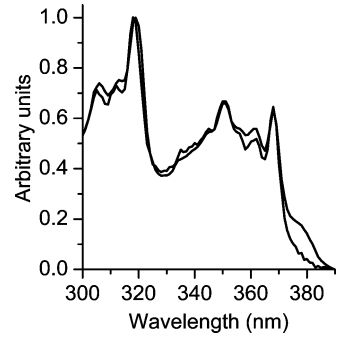

Figure 3. Normalized absorption spectra of PQ in *n*-octane at concentrations of $2 \cdot 10^{-4}$ M (black line) and $1 \cdot 10^{-5}$ M (dark gray line), at room temperature.

To distinguish between monomeric and dimeric PQ species, also the concentration effect on the absorption spectrum in pure *n*-octane was investigated. Figure 3 shows the absorption spectra of PQ in *n*-octane at two 20-fold different concentrations ($2 \cdot 10^{-4}$ and $1 \cdot 10^{-5}$ M) at room temperature. There is an obvious concentration dependence, which was not noticed in earlier experiments due to the smaller concentration range used previously.[1] At higher concentrations, an additional band at 378 nm shows up while the peak at about 318 nm shifts slightly but significantly to the red. Indeed, these spectral changes are similar to the ones observed after lowering the temperature, shown in Figure 2B.

This similarity in temperature and concentration dependence points to a monomer−dimer equilibrium instead of an equilibrium between two monomeric PQ forms: dimer formation is of course favored at higher concentrations and, in view of entropy effects, also at lower temperatures. Such dimers might for

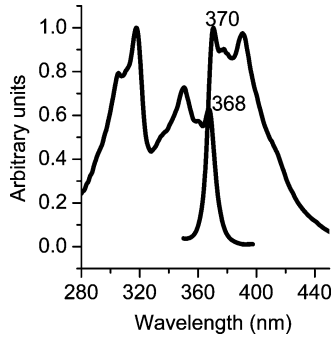

Figure 4. Excitation and emission spectrum of PQ in *n*-octane at room temperature at a concentration of $5 \cdot 10^{-5}$ M.

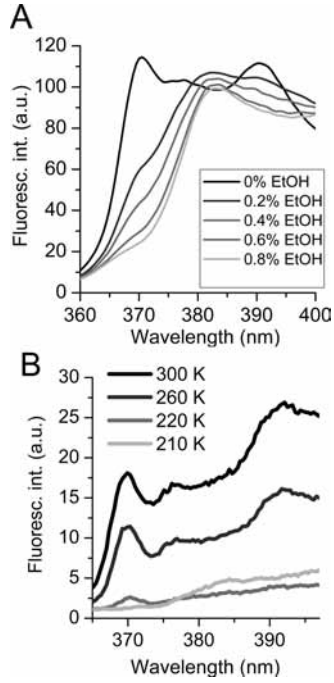

Figure 5. Broad-banded fluorescence emission spectra of PQ with (A) varying traces of ethanol and (B) without added ethanol at temperatures of 300, 260, and 220 K (just above the solidification point) and 210 K (just below the solidification point). The latter curve shows the change in spectral shape upon solidification; for this spectrum the vertical axis does not apply. The spectra in frame A were recorded with lamp excitation at 330 nm and those of frame B using laser excitation at 308 nm. Concn = $5 \cdot 10^{-5}$ M in *n*-octane.

example be stabilized by two H-bonds between N1−H···N2, resulting in a six-membered ring (see Figure 1). Dimers with H-bonds between N1−H···N9 would be less likely because of the lower proton affinity of N9. From Figure 3 and the 290 K curve of Figure 2B, the dimerization constant K_{dim} can be estimated if we assume the extinction coefficient of the dimer to be twice that of the PQ:ethanol complex: $\varepsilon_{dim} = 6 \times 10^3$ M^{-1} cm^{-1}. In that case we calculate $K_{dim} = [PQ:PQ]/[PQ]^2 = 2 \times 10^3$ M^{-1}.

Fluorescence Properties of PQ. In contrast with the findings in absorption, in fluorescence the PQ−ethanol complexes and the PQ dimers behave differently. The fluorescence excitation and emission spectra of $5 \cdot 10^{-5}$ M PQ in *n*-octane (i.e., monomer) at room temperature are shown in Figure 4. Addition of ethanol results in a decrease in intensity of the emission band at 370 nm combined with an increase of the emission of a band at 383 nm (Figure 5, top). The fluorescence excitation spectra (not shown) are very similar to the absorption spectra of Figure 2A. Apparently, the H-bonded PQ/EtOH complex fluoresces and its (0,0) transition is red-shifted to ∼379 nm. On the other hand, for PQ in pure *n*-octane at higher concentrations or at lower temperatures, this additional band at 383 nm is not observed in fluorescence. During cooling the total fluorescence emission intensity of the liquid-state spectra decreases, without changing the spectral shape (Figure 5B). Apparently, in contrast with PQ−ethanol complexes, PQ dimers in *n*-octane exhibit a very low fluorescence quantum yield.

During the cooling process, the properties of a solution of PQ in *n*-octane change dramatically. Cooling PQ in liquid *n*-octane to 220 K shifts the monomer−dimer equilibrium almost completely to the dimer (see also Figure 2B), and upon further cooling below the *n*-octane freezing point (216 K), the monomer emission band at 370 nm completely disappears (Figure 5B). This means that below the freezing point, the concentration of the monomer is beyond detection. Interestingly, under these conditions a weak red-shifted emission is observed with a band at 383 nm (Figure 5B). This emission can either originate from PQ dimers or from PQ complexes with very low concentrations of protic sample impurities (their influence being beyond detection in absorption spectroscopy at room temperature). For three very low concentrations of ethanol (0.001−0.1%), the temperature dependence was investigated (Figure 6). Despite these low concentrations, at temperatures close to the freezing point complex formation with PQ might be significant since under these conditions the solubility of PQ in *n*-octane will be strongly reduced. The weak emission at 383 nm observable in Figure 5 is comparable with the intensity obtained after addition of 0.001% of EtOH in Figure 6. Other alcohols were found to have a comparable effect as that of ethanol (not shown). This indicates that the emission band at 383 nm can be assigned to a PQ solvent impurity complex and that presumably the fluorescence quantum yield of the dimers is fully negligible, even under cryogenic conditions.

Structure of the PQ Dimer. Figures 2 and 3 show that the absorption spectrum of the PQ dimer is very similar to that of the PQ/EtOH complexes, and that there is only a modest red-shift and broadening in comparison with the spectrum of the monomer. This indicates that in the dimer the chromophores are only weakly interacting (a stacked configuration with strong electronic interactions between the π-systems would result in broad, strongly red-shifted absorption spectra which is not the case). Figure 1 shows two possible planar conformations, one in which two H-bonds form a six-membered ring between N1−H···N2 and the other with the H-bonds in an eight-membered ring between N1−H···N9 (see Figure 1). The latter is less likely because of the lower proton affinity of N9.[1] To obtain more information about the nature of the dimer, high-resolution spectroscopy experiments were carried out.

High-resolution Shpol'skii fluorescence spectroscopy can be used to distinguish between spectrally similar tautomers, solvent complexes, and/or dimers,[12−14] provided that these species can be trapped in a polycrystalline matrix under cryogenic conditions. For PQ this was achieved using *n*-octane at 5 K (Figure 7). At the onset of the measurement, the spectrum did not reveal any emission in the 371 nm region, in line with the 210 K spectrum depicted in Figure 5; only some weak emission with sharp peaks at 381.0 and 382.5 nm was observed (Figure 7A). However, illumination of the sample with the laser (nonselective excitation at 308 nm) resulted in a remarkable change in the Shpol'skii spectrum: gradually over time three sharp emission bands with 0−0 transitions at 370.50, 370.75, and 371.48 nm appeared (Figures 7B and 8). All these transitions have the same vibronic structure (verified using site-selective laser excitation,

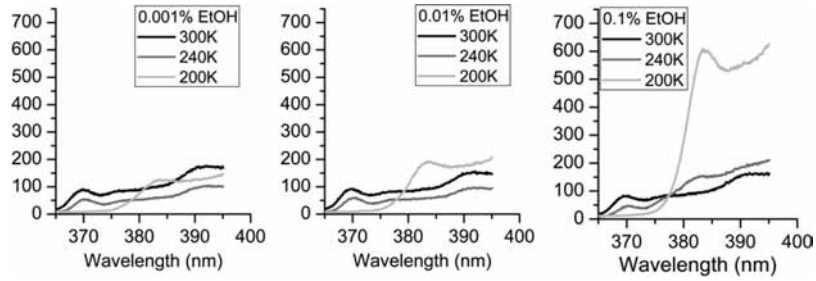

Figure 6. Influence of ethanol, added at 0.001%, 0.01%, and 0.1% levels. Broad-banded fluorescence emission spectra of PQ in *n*-octane excited with the laser at 308 nm at different temperatures. The 200 K spectra show the change in spectral shape upon solidification; for these spectra the vertical axis does not apply.

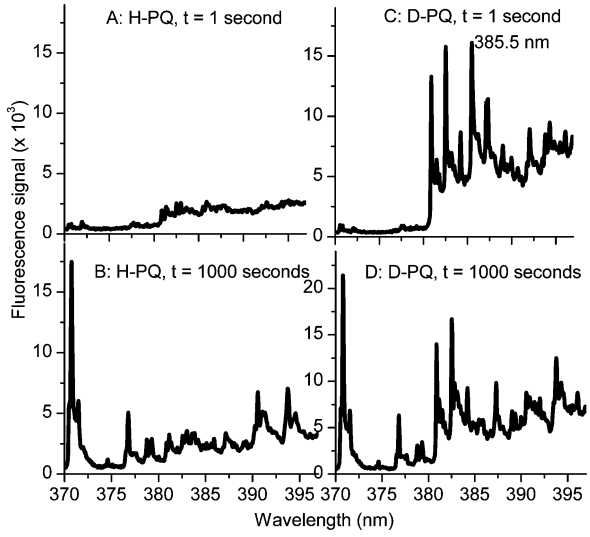

Figure 7. Photochemical conversion: Shpol'skii spectra of nondeuterated (left frames) and deuterated (right frames) PQ samples at 5 K; concn $5 \cdot 10^{-5}$ M in *n*-octane. Laser excitation at 308 nm; the top spectra were recorded during the first second, the bottom spectra after 1000 s of irradiation (also with 1 s of signal accumulation).

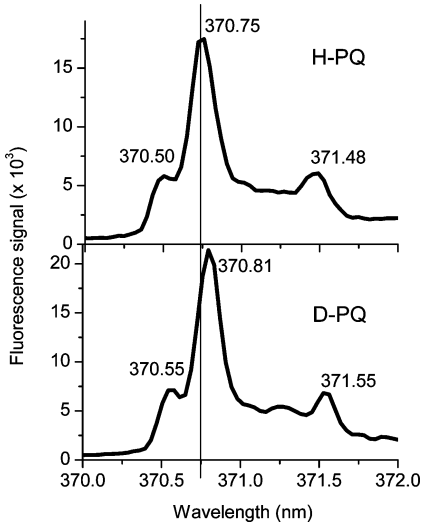

Figure 8. Shpol'skii spectra, showing the 0,0 origin multiplet region of spectra 7B and D on an expanded wavelength scale. Nondeuterated and deuterated PQ in *n*-octane at 5 K, after 1000 s of illumination with an XeCl excimer laser at 308 nm. Note the small but significant red-shift of the *D*-PQ lines relative to those of *H*-PQ.

not shown), and therefore they correspond to the same species, embedded in different crystalline sites. Comparison with the room temperature fluorescence spectrum (Figure 4; 0,0 at 370 nm) suggests that the photoproduct should be identified as the

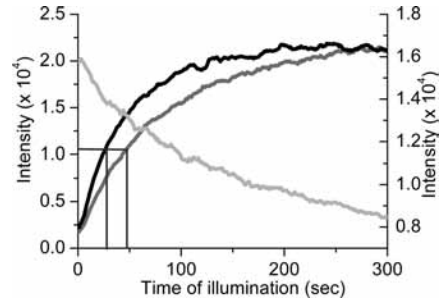

Figure 9. Intensity of the (0,0) transition at 370.75 nm of *H*-PQ (black curve) and that of *D*-PQ at 370.81 nm (dark gray curve) as a function of irradiation time (excimer laser, 308 nm). The light gray curve (right axis) shows the decreasing (0,0) band of the *D*-PQ dimer at 385.5 nm.

PQ monomer, the predominant species at room temperature. Its rate of formation during illumination (half-life time approximately 28 s) is depicted in Figure 9. The photoproduct disappeared when the sample was subsequently heated to approximately 100 K and reappeared (with roughly the same intensity) only after cooling back to below 40 K and subsequent laser (or lamp) illumination.

The gradual increase in intensity of the PQ monomer fluorescence with (0,0) transitions around 371 nm is not accompanied by a measurable reduction of the emission elsewhere in the spectrum (compare Figure 7A and B). Apparently, it is formed from a nonfluorescent species. The photon-induced conversion is only observed at very low temperatures, and apparently the product is not stable at temperatures higher than about 40 K. Furthermore, this process is reversible upon heating and cooling the sample, which means that the photoreactive species is not chemically decomposed. This suggests that the photoreactive species is the nonfluorescent dimer of PQ, whereas the persisting weak lines in the 381−383 nm range are due to PQ-impurity complexes.

How can one explain the negligible fluorescence quantum yield of the dimer and its photochemical transformation to a strongly emitting monomer, even in a rigid matrix at 5 K, where substantial molecular rearrangements will be inhibited? Our hypothesis is that excited-state double proton transfer (ESDPT) in PQ dimers plays a major role, a process that requires only minor structural changes in the dimer conformation. In ESDPT two protons are transferred, leading to the formation of an excited dimer of tautomers. As demonstrated for $(7\text{-AI})_2$, the process can take place in a concerted or in a stepwise fashion.[15] It causes efficient fluorescence quenching assuming that the tautomeric dimer species formed upon ESDPT is nonfluorescent. In $(7\text{-AI})_2$ at 5 K this process follows a tunneling mechanism,[15] so that its rate is strongly dependent on the barrier width, in other words on the exact dimer configuration. Even a minor

photochemical rearrangement of this configuration will impede the ESDPT process so that the PQ monomer emission will no longer be fully quenched.

To check this hypothesis, the Shpol'skii experiments were repeated using deuterated PQ. Deuteration is expected to have a strong effect on ESDPT, since under cryogenic conditions (5 K) deuteron tunneling is much slower than proton tunneling.[15,16] This means that in *D*-PQ dimers, excited-state double deuteron transfer (ESDDT) may take place on a time scale similar to or perhaps even slower than that of fluorescence emission, so that dimer fluorescence should be expected. In Figure 7C and D two Shpol'skii spectra of *D*-PQ in *n*-octane at 5 K are shown, recorded during the first second and after 1000 s of irradiation at 308 nm. The difference between these spectra and those of *H*-PQ is striking: at the onset of the experiment for the deuterated system intense high-resolution fluorescence emission is observed with strong, sharp features in the 380−385 nm range. During illumination, the monomeric species *D*-PQ with (0,0) transitions at 370.55, 370.81, and 371.55 nm is formed, very close but not identical to those observed for *H*-PQ (see Figure 8; the red shift of 4−5 cm^{-1} upon deuteration is due to small diferences in zero-point energy, as explained by Bader and co-workers[16]). However, in the deuterated system the fluorescent monomer is not formed from a dark species; the increase of this monomer spectrum is accompanied by the decrease of the 385.5 nm line, as visualized in Figure 9. In the 1000 s spectrum in Figure 7D, this line has fully disappeared. The increase at 370.8 nm and the decrease at 385.5 nm show similar half-life times of approximately 48 s; both are slower than the increase at 370.75 nm (half-life time ca. 28 s) observed for *H*-PQ under identical irradiances.

It should be emphasized that the experimental conditions for recording the spectra for *H*-PQ and *D*-PQ in Figure 7 were fully identical: the same PQ solution in *n*-octane was exposed to the same volume of H_2O/D_2O, and the resulting samples were cooled together and analyzed in one series. Consequently, the concentrations of *H*-PQ and *D*-PQ were the same, as well as the levels of possible protic impurities. The remarkable differences between Figure 7A, B and Figure 7C, D should therefore completely be ascribed to the difference between ESDPT and ESDDT.

Figure 7C shows three intense lines in the 380−385 nm region, some 10 nm red-shifted compared to the emission of the monomer, as expected in view of the broad emission band of Figure 5B. Only one of these species (with the emission band at 385.5 nm) can be photoconverted to a monomer; the other two are not affected by irradiation. As will be discussed below, this is not unexpected since the required structural rearrangement at 5 K in a crystalline matrix is not trivial and will be largely conformation dependent. The lines at 381.0 and 382.5 nm could therefore correspond to dimers in a conformation or crystalline site that does not allow this type of photolysis, or in which the photoproduct can revert too quickly to the dimeric species.

Photochemical Production of the Monomer. WIth regard to the photochemical reaction leading to monomer emission, it should be realized that not a complete dissociation is required—impossible in crystalline *n*-octane matrices at 5 K—but only a minor change of the dimer configuration. If we denote the ground-state dimer as NN (two interacting molecules in their normal tautomeric form), such a separated species can be indicated by N--N. The energy barrier between the NN and N--N form is low and is only significant at cryogenic temperatures. Already upon warming up the sample to about 40 K, the pair is converted to NN again.

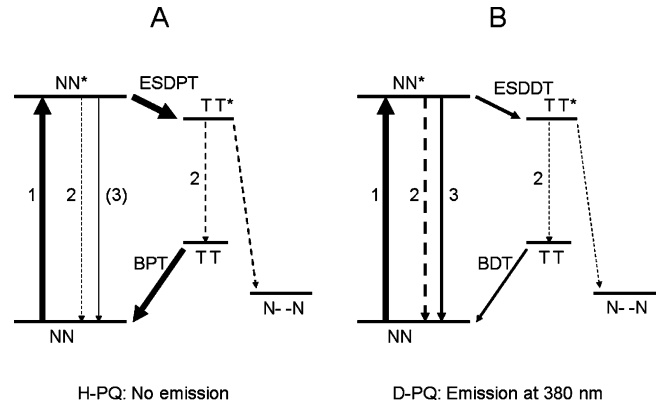

Figure 10. Simplified kinetic model to explain the photochemical and photophysical behavior of *H*-PQ (A) and *D*-PQ dimers (B). The line thicknesses of the arrows indicate the relative overall efficiencies for the various processes: absorption (1), nonradiative decay (2), and radiative decay (3) excited-state double proton/deuteron transfer (ESDPT/ESDDT), back proton/deuteron transfer (BPT/BDT), and the formation of two separate monomers.

Figure 9 reveals that the half-life times of formation of the 0−0 lines are about 28 s (1*H*-PQ) and 48 s (1*D*-PQ), differing by roughly a factor of 2. In separate experiments, similar formation rates of the 1*H*-PQ monomer were observed with dye laser excitation in the 0−0 region of the dimer (360−385.5 nm) or slightly slower using Xe-lamp excitation at 330 nm. Since the electronic states involved with *H*-PQ and *D*-PQ will be very similar in energy, the difference in the photochemical and photophysical behavior is explained with a simplified kinetic model (see Figure 10). The starting population of the ground-state NN is obviously the same for both compounds. After excitation, species NN* is formed. For *H*-PQ this state has a very short lifetime because of fast ESDPT so that its fluorescence quantum yield from NN* is negligible and TT* (TT denotes both molecules existing in the tautomeric forms other than 1*H*-PQ) is formed in an almost 100% yield. For *D*-PQ, however, the rate constant of ESDDT is reduced, which results in a much longer lifetime of NN*. The fact that the photoreaction is not much faster but slightly slower for *D*-PQ suggests that NN* is not the reactive species. If we assume ESDDT to be roughly as fast as internal conversion and fluorescence from NN* combined, the yield in TT* states for *D*-PQ would be about half that of the TT* yield of *H*-PQ. The observed twofold difference in photochemistry rate (half-life times 48 vs 28 s; see Figure 9) would agree with TT* being the reactive species. Apart from internal conversion to TT, this TT* state can decay to N--N, presumably via an intermediate T--T state of which the conformation has undergone sufficient changes to preclude return to the TT or NN state in the 5 K matrix. The exact nature of these conformational changes is currently unknown; the excess of vibrational energy upon excitation may play a role here. TT turns into NN via back proton/deuteron transfer (BPT/BDT). The NN dimer and N--N photolytic product are separated by a very low energy barrier; at temperatures above 40 K the system reverts to NN.

In other words, the results obtained can be rationalized on the basis of the scheme in Figure 10, assuming that the photochemical rearrangement starts in the TT* excited state. This is not unreasonable since its optimal structure (the tautomer having the structure of 2*H*-PQ, see Figure 1) will be quite different from that of NN (the monomer having the structure of 1*H*-PQ). Thus, the photochemical process might follow the following schedule:

$$TT^* \rightarrow T\text{--}T \rightarrow N\text{--}N$$

where the fluorescence of N--N is regarded as monomeric.

To summarize, the involvement of excited-state double proton transfer can explain the lack of fluorescence of the *H*-PQ dimer, the observation of fluorescence of the deuterated dimer, and the gradual appearance of PQ monomer fluorescence during irradiation in a low-temperature matrix. Unfortunately, a detailed kinetic analysis is not possible since not only the normal dimer of *H*-PQ but also the TT* forms (both for *H*-PQ and *D*-PQ) are nonfluorescent.

Conclusions

In the above study the extraordinary photophysical and photochemical behavior of PQ in *n*-octane has been elucidated. In such samples one deals with fluorescent monomers, nonfluorescent dimers, and possibly also fluorescent complexes with H-bonding impurities. As indicated by the ethanol addition experiments, very low concentrations of such impurities already suffice to produce such complexes (0.2% in case of ethanol). In pure *n*-octane the equilibrium between monomer and dimer shifts to the dimer at lower temperatures as well as at higher concentrations. As a result, the fluorescence intensity of a PQ solution decreases during cooling.

In frozen *n*-octane (before irradiation), only the dimer is present so that no fluorescence is observed. We observe only a weak emission that is attributed to PQ-impurity complexes. In the PQ dimer the fluorescence from NN* is fully quenched because of very fast excited-state intermolecular double proton transfer (ESIDPT), resulting in a new nonfluorescent dimer of tautomers TT*. Deuteration experiments confirmed this mechanism: in a *D*-PQ frozen solution at very low temperatures (5 K), dimer emission is observed. In the deuterated dimer the fluorescence from NN* is not fully quenched because deuteron transfer is much slower than proton transfer. The ESIDPT process is qualitatively similar to that described for 7AI,[7,10] but in the case of PQ we assume the double hydrogen bond to form a six-membered ring.

Irradiation of PQ in a crystalline *n*-octane matrix under cryogenic conditions induces a reversible photolysis of the dimeric "dark" species. It requires a minor rearrangement of the dimer structure so that the ESIDPT process is sufficiently slowed down and a strong monomer-type fluorescence can be observed. The wavelength of the (0,0) transition agrees with that observed for the monomer in room temperature solutions. In the photolyzed dimer, the monomers are separated by a low barrier: at temperatures above 40 K the dimer structure is restored so that the emission at 370 nm disappears. This emission reappears again upon cooling to 5 K and irradiation, which underscores the reversibility of the process.

Acknowledgment. The research visits of S. Zapotoczny and M. Sterzel to LCVU Amsterdam were supported by the European Commission (Large-Scale Research Infrastructures program, contract no. HPRI-CT-1999-00064). We thank Milio de Charro for help with the low-temperature absorption and fluorescence measurements and Joost Buijs for technical support.

References and Notes

(1) Zapotoczny, S.; Danel, A.; Sterzel, M. T.; Pilch, M. *J. Phys. Chem. A* **2007**, *111*, 5408–5414.
(2) Musierowicz, A.; Niementowski, S.; Tomasik, Z. *Rocz. Chem.* **1928**, *8*, p. 325.
(3) Rechthaler, K.; Rotkiewicz, K.; Danel, A.; Tomasik, P.; Khatcharian, K.; Kohler, G. *J. Fluoresc.* **1997**, *7*, p. 301.
(4) Rurack, K.; Danel, A.; Rotkiewicz, K.; Grabka, D.; Spieles, M.; Rettig, W. *Org. Lett.* **2002**, *4*, p. 4647.
(5) Pan, J.-H.; Chou, Y.-M.; Chiu, H.-L.; Wang, B.-C. *Tamkang J. Sci. Eng.* **2005**, *8*, p. 175.
(6) Nakajima, A.; Hirano, M.; Hasumi, R.; Kaya, K.; Watanabe, H.; Carter, C. C.; Williamson, J. M.; Miller, T. A. *J. Phys. Chem.* **1997**, *101*, 392–398.
(7) Chachisvilis, M.; Fiebig, T.; Douhal, A.; Zewail, A. H. *J. Phys. Chem. A* **1998**, *102*, 669–673.
(8) Danel, A.; Zapotoczny, S.; Sterzel, M. T.; Pilch, M. *J. Mol. Struct.* **2004**, *682*, 179–183.
(9) Gooijer, C.; Ariese, F.; Hofstraat, J. W. *Shpol'skii Spectroscopy and Other Site-Selection Methods*; Wiley Interscience: New York, 2000.
(10) Catalan, J.; Kasha, M. *J. Phys. Chem. A* **2000**, *104*, 10812–10820.
(11) Paul, S.; Gupta, M.; Gupta, R.; Loupy, A. *Tetrahedron Lett.* **2001**, *42*, 3827.
(12) Bader, A. N.; Ariese, F.; Gooijer, C. *J. Phys. Chem. A* **2002**, *106*, 2844–2849.
(13) Bader, A. N.; Pivovarenko, V.; Demchenko, A. P.; Ariese, F.; Gooijer, C. *Spectrochim. Acta, Part A* **2003**, *59*, 1593–1603.
(14) de Klerk, J. S.; Szemik-Hojniak, A.; Ariese, F.; Gooijer, C. *Spectrochim. Acta, Part A* **2009**, *72*, 144–150.
(15) Kwon, O.-H.; Zewail, A. H. *Proc. Natl. Acad. Sci. U.S.A.* **2007**, *104* (21), 8703–8708.
(16) Bader, A. N.; Pivovarenko, V.; Demchenko, A. P.; Ariese, F.; Gooijer, C. *J. Phys. Chem. B* **2004**, *108*, 10589–10595.

JP8086545